Research Article
Molecular and Cell Biology

JOURNAL
OF HEPATOLOGY

Loss of fibrocystin promotes interleukin-8-dependent proliferation and CTGF production of biliary epithelium

Graphical abstract

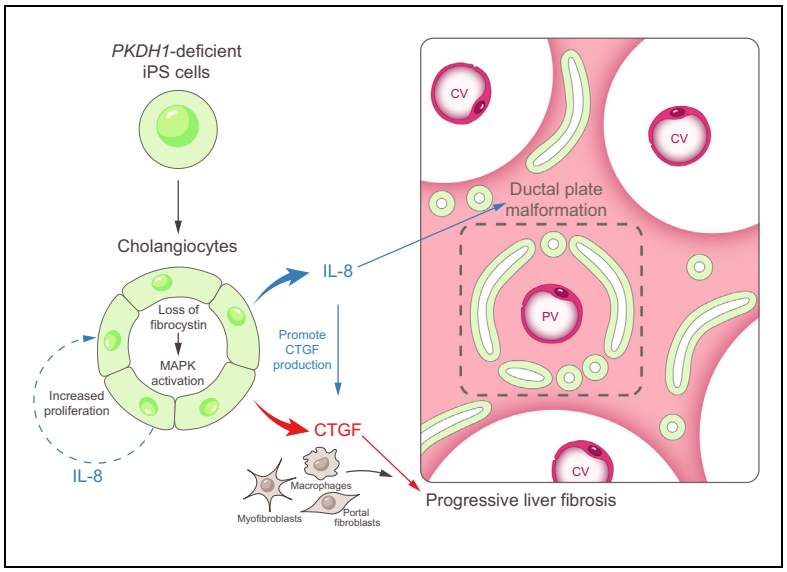

Highlights

- We established a human iPS cell-model of congenital hepatic fibrosis.
- Loss of fibrocystin increases the production of IL-8 in cholangiocytes.
- The proliferation of fibrocystin-deficient cholangiocytes and their production of CTGF are increased in an IL-8-dependent manner.
- Expression of IL-8 and CTGF is increased in the livers of patients with congenital hepatic fibrosis.

Authors

Tomoyuki Tsunoda, Sei Kakinuma, Masato Miyoshi, ..., Hiromitsu Nakauchi, Yasuhiro Asahina, Mamoru Watanabe

Correspondence

skakinuma.gast@tmd.ac.jp
(S. Kakinuma) asahina.gast@tmd.ac.jp
(Y. Asahina) mamoru.gast@tmd.ac.jp
(M. Watanabe)

Lay summary

Congenital hepatic fibrosis (CHF) is a genetic liver disease caused by mutations of the *PKHD1* gene. Dysfunction of the protein it encodes, fibrocystin, is closely associated with CHF pathogenesis. Using an *in vitro* human induced pluripotent stem cell model and patient samples, we showed that the loss of fibrocystin function promotes proliferation of cholangiocytes and the production of connective tissue growth factor (CTGF) in an interleukin 8 (IL-8)-dependent manner. These results suggest that IL-8 and CTGF are essential for the pathogenesis of CHF.

http://dx.doi.org/10.1016/j.jhep.2019.02.024
 J. Hepatol. 2019, 71, 143–152

Research Article
Molecular and Cell Biology

JOURNAL OF HEPATOLOGY

Loss of fibrocystin promotes interleukin-8-dependent proliferation and CTGF production of biliary epithelium

Tomoyuki Tsunoda[1,†], Sei Kakinuma[1,2,*,†], Masato Miyoshi[1], Akihide Kamiya[3], Shun Kaneko[1], Ayako Sato[1], Jun Tsuchiya[1], Sayuri Nitta[1], Fukiko Kawai-Kitahata[1], Miyako Murakawa[1], Yasuhiro Itsui[1], Mina Nakagawa[1], Seishin Azuma[1], Tsuyoshi Sogo[4], Haruki Komatsu[5], Ryutaro Mukouchi[6], Ayano Inui[4], Tomoo Fujisawa[4], Hiromitsu Nakauchi[7,8], Yasuhiro Asahina[1,2,*], Mamoru Watanabe[1,*]

[1]*Department of Gastroenterology and Hepatology, Tokyo Medical and Dental University (TMDU), Tokyo, Japan;* [2]*Department of Liver Disease Control, Tokyo Medical and Dental University (TMDU), Tokyo, Japan;* [3]*Department of Molecular Life Sciences, School of Medicine, Tokai University, Isehara, Japan;* [4]*Department of Pediatric Hepatology and Gastroenterology, Saiseikai Yokohamashi Tobu Hospital, Yokohama, Japan;* [5]*Department of Pediatrics, Toho University Sakura Medical Center, Sakura, Japan;* [6]*Department of Pathology, Saiseikai Yokohamashi Tobu Hospital, Yokohama, Japan;* [7]*Institute for Stem Cell Biology and Regenerative Medicine, Stanford University School of Medicine, Stanford, CA, USA;* [8]*Division of Stem Cell Therapy, Institute of Medical Science, The University of Tokyo, Tokyo, Japan*

Background & Aims: Congenital hepatic fibrosis (CHF) is a genetic liver disease resulting in abnormal proliferation of cholangiocytes and progressive hepatic fibrosis. CHF is caused by mutations in the *PKHD1* gene and the subsequent dysfunction of the protein it encodes, fibrocystin. However, the underlying molecular mechanism of CHF, which is quite different from liver cirrhosis, remains unclear. This study investigated the molecular mechanism of CHF pathophysiology using a genetically engineered human induced pluripotent stem (iPS) cell model to aid the discovery of novel therapeutic agents for CHF.

Methods: *PKHD1*-knockout (*PKHD1*-KO) and heterozygously mutated *PKHD1* iPS clones were established by RNA-guided genome editing using the CRISPR/Cas9 system. The iPS clones were differentiated into cholangiocyte-like cells in cysts (cholangiocytic cysts [CCs]) in a 3D-culture system.

Results: The CCs were composed of a monolayer of cholangiocyte-like cells. The proliferation of *PKHD1*-KO CCs was significantly increased by interleukin-8 (IL-8) secreted in an autocrine manner. IL-8 production was significantly elevated in *PKHD1*-KO CCs due to mitogen-activated protein kinase pathway activation caused by fibrocystin deficiency. The production of connective tissue growth factor (CTGF) was also increased in *PKHD1*-KO CCs in an IL-8-dependent manner. Furthermore, validation analysis demonstrated that both the serum IL-8 level and the expression of *IL-8* and *CTGF* in the liver samples were significantly increased in patients with CHF, consistent with our *in vitro* human iPS-disease model of CHF.

Conclusions: Loss of fibrocystin function promotes IL-8-dependent proliferation of, and CTGF production by, human cholangiocytes, suggesting that IL-8 and CTGF are essential for the pathogenesis of CHF. IL-8 and CTGF are candidate molecular targets for the treatment of CHF.

Lay summary: Congenital hepatic fibrosis (CHF) is a genetic liver disease caused by mutations of the *PKHD1* gene. Dysfunction of the protein it encodes, fibrocystin, is closely associated with CHF pathogenesis. Using an *in vitro* human induced pluripotent stem cell model and patient samples, we showed that the loss of fibrocystin function promotes proliferation of cholangiocytes and the production of connective tissue growth factor (CTGF) in an interleukin 8 (IL-8)-dependent manner. These results suggest that IL-8 and CTGF are essential for the pathogenesis of CHF.

Introduction

Congenital hepatic fibrosis (CHF) is a rare genetic liver disease (1/20,000 births) characterized by ductal plate malformation during bile duct development and progressive hepatic fibrosis. CHF is also frequently associated with autosomal recessive polycystic kidney disease.[1] Liver transplantation is necessary for the treatment of patients with progressive CHF and a severe phenotype. There is lots of pathological evidence to indicate that the mechanism of fibrosis in CHF is quite different from liver cirrhosis due to chronic hepatitis: in patients with CHF, neither necroinflammatory changes in hepatocytes nor hepatic stellate cell activation are observed. Fibrotic change in the CHF liver is limited to periportal areas of the hepatic lobes and is not observed around the central vein.[2] The pathophysiology of ductal plate malformation and progressive fibrosis in the CHF liver remains unclear.

Keywords: Polycystic kidney and hepatic disease 1; PKHD1; Fibrocystin; Congenital hepatic fibrosis; Human induced pluripotent stem cells; Hepatic progenitor-like cells; Ductal plate malformation; Liver transplantation.
Received 9 November 2018; received in revised form 6 February 2019; accepted 14 February 2019; available online 19 March 2019

* Corresponding authors. Address: Department of Gastroenterology and Hepatology, Tokyo Medical and Dental University, 1-5-45 Yushima, Bunkyo-ku, Tokyo 1138519, Japan. Tel: +81-3-3813-6111. Fax: +81-3-5803-0268 (S. Kakinuma, Y. Asahina, or M. Watanabe).
E-mail addresses: skakinuma.gast@tmd.ac.jp (S. Kakinuma), asahina.gast@tmd.ac.jp (Y. Asahina), mamoru.gast@tmd.ac.jp (M. Watanabe).
† These authors contributed equally to this work.

Research models using human induced pluripotent stem (iPS) cell-derived hepatic cells have been used to investigate the pathophysiology of various diseases including genetic disorders.[3] Human iPS cell lines derived from patients with genetic diseases are often used to establish the disease models; however, there are some limitations in such studies due to different genetic backgrounds, lack of phenotypic markers, various mutation patterns in disease, and the varied multipotency of iPS cell lines. Therefore, it is reasonable that genetically engineered human iPS cells derived from healthy individuals are used for the study of diseases.[4,5]

PKHD1, the gene responsible for CHF, is a large gene composed of >400,000 bases and >400 mutation patterns have been reported in patients with CHF of different severity.[6–8] It encodes the fibrocystin protein, which is localized in the primary cilia of cholangiocytes.[7–9] The dysfunction of primary cilia lacking fibrocystin was suggested to be essential in the development of CHF. Animal models of CHF, spontaneous mutant polycystic kidney rat and gene-targeted *Pkhd1* mutated mice, have been developed;[10–12] however, there are several phenotypic differences between human CHF and these animal models. The marked infiltration of inflammatory cells around the portal vein, cysts of the pancreatic duct, and dilation of the extrahepatic bile duct are observed in *Pkhd1*-knockout (*PKHD1*-KO) mice, but are rare in patients with CHF, probably because of variations due to species specificity.[10,12] Thus, a disease model using human cells is necessary for the study of CHF pathophysiology. It is difficult to clarify such mechanisms using an iPS-cell model derived from patients with CHF because of the numerous mutation patterns without specific correlation between genetic and phenotype variations. Furthermore, the complete functional loss of fibrocystin is lethal in the fetal period.[13]

In this study, we investigated the pathophysiology of CHF by establishing a human iPS cell model derived from healthy individuals, in which the function of fibrocystin was lost by genome-editing technology, to explore novel therapeutic agents for CHF. Our disease model demonstrated that the loss of fibrocystin in human iPS-derived cholangiocyte-like cells increased the proliferation of such cells in an interleukin-8 (IL-8)-dependent manner via activation of the mitogen-activated protein kinase (MAPK) pathway and promoted the production of connective tissue growth factor (CTGF [or CCN2]). Moreover, the expression of IL-8 and CTGF was increased in the livers of patients with CHF, consistent with the results of the human iPS model. These results indicated that increased IL-8 and CTGF production, caused by the dysfunction of fibrocystin, is essential for the development of bile duct malformation and progressive fibrosis in patients with CHF.

Materials and methods

Generation of *PKHD1* mutant iPS cells

A human iPS cell line, TkDA3-4 clone (established from dermal fibroblasts of a normal healthy human) was cultured using the Cellartis® DEF-CS™ 500 culture system (Takara Bio, Shiga, Japan). Targeted homologous recombination of the gene cassette into TkDA3-4 iPS cells was performed by electroporation (Fig. 1A and Fig. S1A). Briefly, 1×10^6 iPS TkDA3-4 cells were transfected using Lonza 4D-Nucleofector (Lonza, Basel, Switzerland) with 2.5 μg of plasmid expressing Cas9 and gRNA and 2.5 μg of the targeting vector containing a puromycin resistance gene cassette. After electroporation, the cells were immediately resuspended in pre-warmed iPS cell culture medium and then incubated at 37 °C. The culture medium was changed every 24 h after transfection. Puromycin (0.5 μg/ml) was added to the medium from 3 to 6 days after the transfection to select the recombined cells. The clones were picked under a microscope and cultured. The genotype of the clones was determined by PCR (Fig. S1B). Clones carrying the mutant fragment were selected and the DNA sequences of the wild-type fragment were determined by direct sequencing. Clones with a premature stop codon in *PKHD1* exon 2 were selected as the *PKHD1*-KO cell line and the loss of fibrocystin in the KO lines was confirmed by immunostaining. To exclude the possibility that an off-target mutation by the CRISPR/Cas9 genome-editing method affected the phenotype of such clones, 2 different gRNA sequences were used for genome editing, and the phenotype of such cells was analyzed using more than 3 clones derived from genome-edited clones using each gRNA sequence (Figs. S1 A-E, S2A, S2E and S4B). The mutant protein in KO cells was predicted to retain only the first 11 amino acids. More than 3 hepatic progenitor-like cell (HPC) clones derived from 1 *PKHD1*-KO iPS clone were established and were analyzed.

Human samples and ethical statement

Patients with clinically diagnosed congenital hepatic fibrosis and age matched control patients with chronic hepatitis C were recruited in this study. All human samples used in this study were retrospective samples. Liver biopsies were performed for pathological diagnosis or follow-up evaluation with clinical necessity and the remaining formalin fixed paraffin embedded samples were used in this study.

The study protocol conformed to the ethical guidelines of the Declaration of Helsinki and was approved by the institutional ethics committees of Tokyo Medical and Dental University and Saiseikai Yokohamashi Tobu Hospital (authorization number: Tokyo Medical and Dental University M2016-185, Saiseikai Yokohamashi Tobu Hospital 2016085). Written informed consent or informed assent for the use of stored samples was obtained from the patients or their legal guardians.

For further details regarding the materials and methods used, please refer to the CTAT table and supplementary information.

Results

Generation of *PKHD1*-KO iPS-derived hepatic progenitor-like cells as a model for congenital hepatic fibrosis

To delete the function of fibrocystin, exon 2 (start codon) of the *PKHD1* gene was replaced by a targeting gene cassette in a human iPS cell line (derived from a healthy human, TkDA3-4 clone) using CRISPR/Cas9 genome-editing methods (Fig. 1A). Heterozygously mutated *PKHD1* (*PKHD1*-Hetero) iPS clones obtained using same gRNA as *PKHD1*-KO iPS clones were used as control cell lines in this study to exclude the possibility that an off-target mutation by the genome-editing method affected the phenotype of such clones. The loss of fibrocystin in *PKHD1*-KO iPS clones was validated by immunostaining for fibrocystin (Fig. 1B). Fluorescence-activated cell sorting and quantitative reverse transcription (RT-qPCR) analysis demonstrated that the expression of TRA-1-60, SSEA-4, NANOG, and OCT3/4 (or POU5FI) in *PKHD1*-KO clones were similar between WT and *PKHD1*-Hetero clones (Fig. 1C and S1). These data indicated that the pluripotency of such iPS clones was maintained.

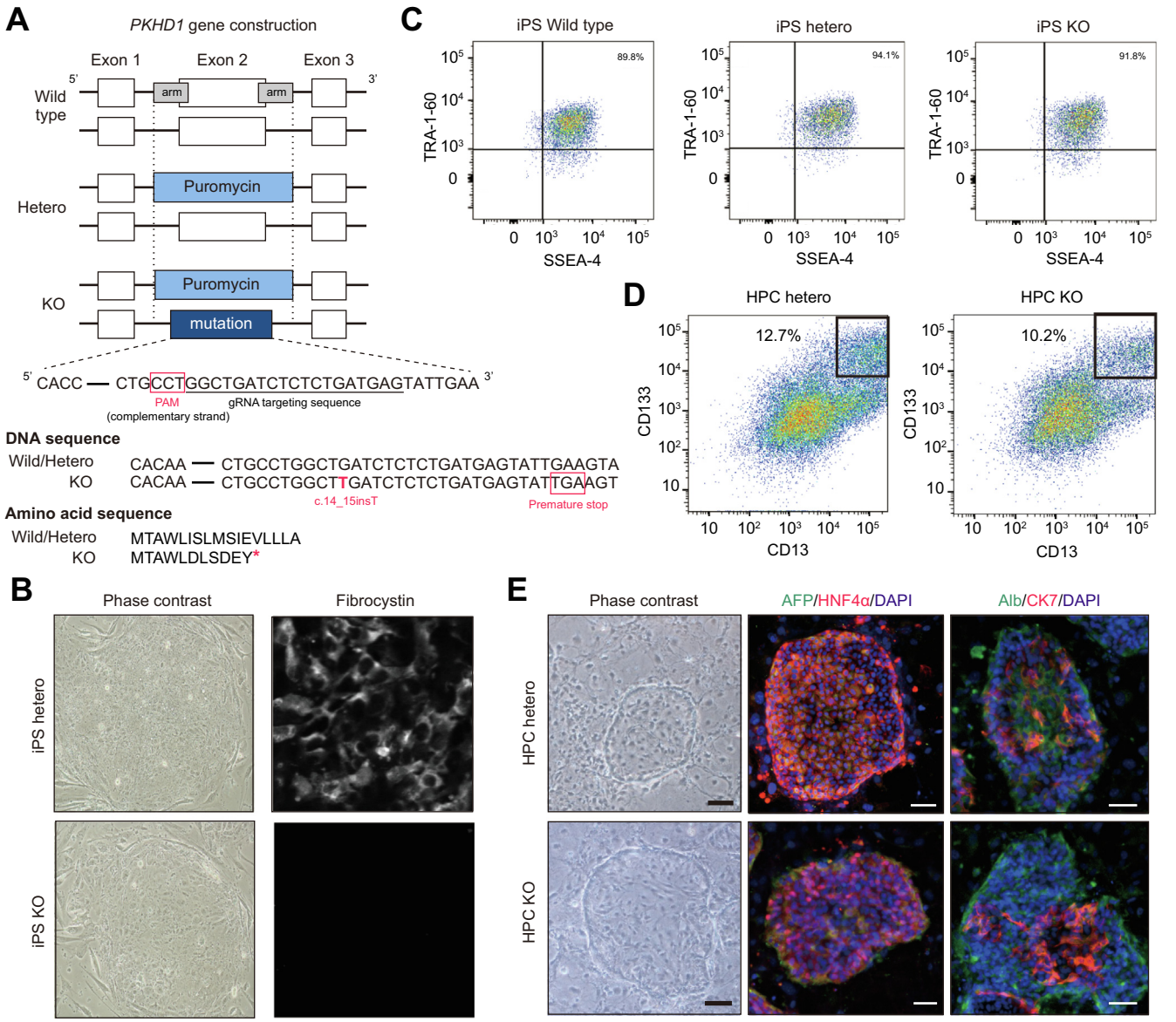

Fig. 1. Generation of *PKHD1*-KO iPS-derived hepatic progenitor-like cells. (A) Gene construction of targeting vector and guide RNA. A PAM sequence (surrounded by square) was designed on exon 2 of *PKHD1*. A DNA allele not replaced by the puromycin cassette had the c.14_15 insT point mutation, which resulted in a premature stop codon in KO clones. (B) Immunostaining of fibrocystin in human iPS cell-colonies. *PKHD1*-KO iPS cells lacked fibrocystin protein. (C) Representative flow cytometric analysis of SSEA-4 and TRA-1–60 cells in heterozygous and *PKHD1*-KO iPS cells. (D) Expression of hepatic progenitor markers, CD13 and CD133, in human iPS cells during differentiation into the hepatic lineage. (E) Immunostaining of AFP (green), HNF4α (red), Alb (green), and CK7 (red). Nuclei were stained with DAPI (blue). HPC formed large colonies expressing both hepatocytic and cholangiocytic markers on feeder cells. Scale bars: 10 μm. AFP, α-fetoprotein; Alb, albumin; HNF4α, hepatic nuclear factor 4 α, HPC, hepatic progenitor-like cell; iPS, induced pluripotent stem; *PKHD1*-KO, *PKHD1* knockout. (This figure appears in colour on the web.)

Next, *PKHD1*-KO or *PKHD1*-Hetero iPS clones were differentiated into the hepatic lineage, and the $CD13^{high}CD133^{+}$ cell fraction in the cultured cells was sorted onto feeder cells as previously described (Fig. 1D).[14] Clones of these cells were stably maintained and cultured as iPS cell-derived hepatic progenitor-like cells (iPS-HPCs), which expressed both hepatocytic and cholangiocytic markers (Fig. 1E).

Loss of PKHD1 increases the cell proliferation of iPS-derived cholangiocytic cysts

To evaluate the phenotype of *PKHD1*-KO cells in the biliary lineage, we employed a 3D-culture system as previously described.[14] In this culture system, iPS-HPC-derived cells form cyst-like structures exhibiting the characteristics of cholangiocytes and cell polarity, termed cholangiocytic cysts (CCs, Fig. 2A and S2A). CCs were composed of a monolayer of cytokeratin (CK) 7-positive cells with clear luminal spaces and cell polarity, where F-actin was located at the apical membrane and β-catenin was present at the basolateral side (Fig. 2B). Fibrocystin was expressed on the luminal side in *PKHD1*-Hetero CCs (Fig. 2B). Human iPS-derived CCs transport rhodamine 123, a substrate for MDR1 (also called ABCB1), from the basal to the apical side (Fig. 2C, left panel), demonstrating that iPS-derived cholangiocyte-like cells in cysts exhibit both the structural and functional characteristics of cholangiocytes.

Gene expression related to cholangiocytic differentiation, including *CK19* (or *KRT19*), Jagged1/2 (*JAG1/2*), hepatic nuclear factor (*HNF*)*1β*, and sex determining region Y-box 9 (*SOX9*) in

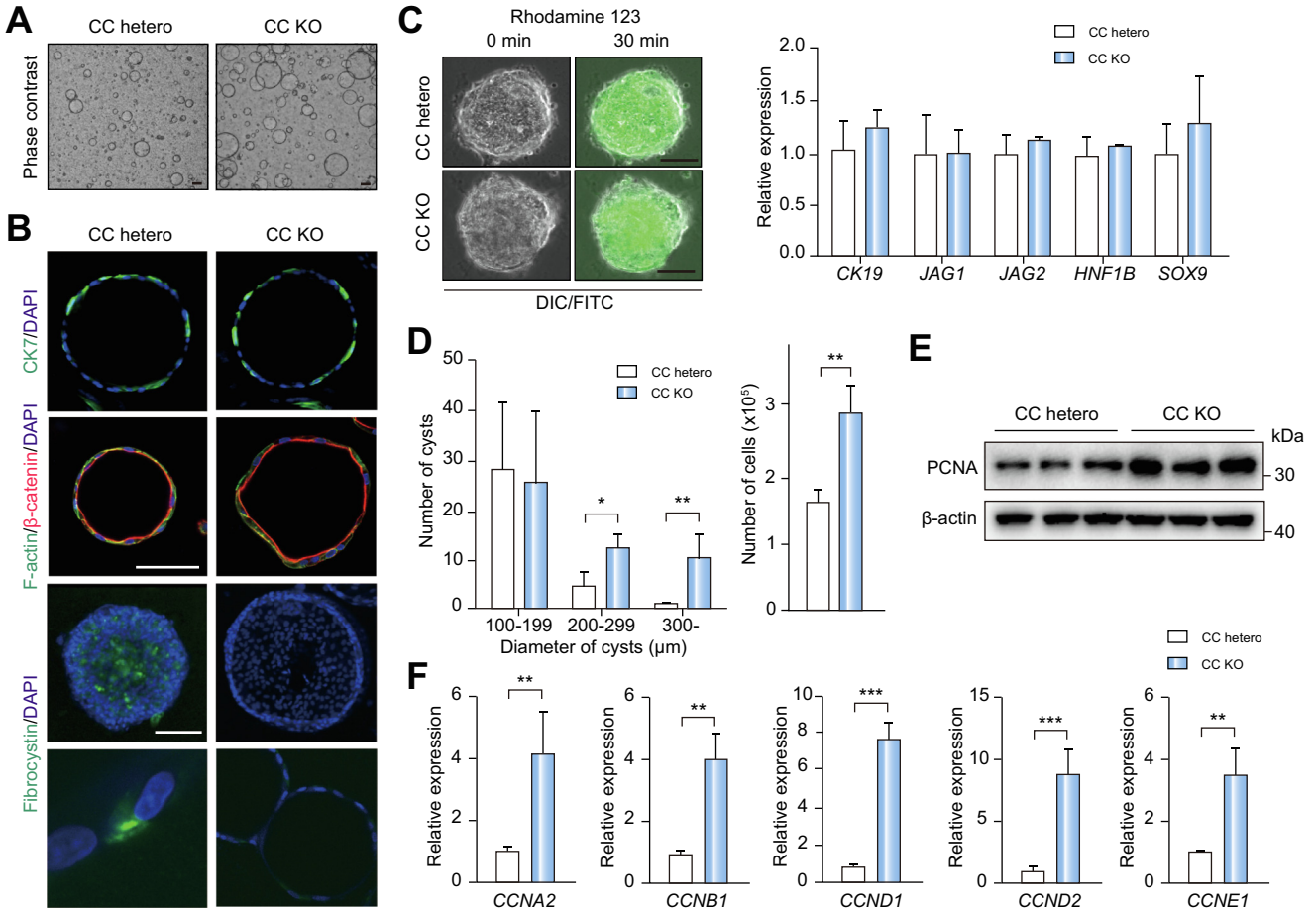

Fig. 2. Loss of PKHD1 promotes the proliferation of iPS-derived cholangiocytes in cysts. (A) Representative images of CCs derived from heterozygous and *PKHD1*-KO iPS cells. Scale bars: 100 μm. (B) Immunostaining of CK7 (green), F-actin (green), β-catenin (red), and fibrocystin (green). Nuclei were counterstained with DAPI (blue). Scale bars: 10 μm (upper-right panel) and 100 μm (other panels). (C) Rhodamine 123 was transported into the apical side of *PKHD1*-Hetero and *PKHD1*-KO CCs from the basal side, indicating the functional transport ability of CCs (left panel). Scale bars: 50 μm. RT-qPCR analysis of *CK19*, *JAG1*, *JAG2*, *HNF1β*, and *SOX9* in *PKHD1*-Hetero and *PKHD1*-KO CCs (right panel). (D) Numbers of *PKHD1*-Hetero and *PKHD1*-KO CCs (diameter >100 μm with clear lumina) in 3D-culture/well (left panel). Number of cells composed in the CCs (right panel). (E) Immunoblot of PCNA in *PKHD1*-Hetero and *PKHD1*-KO CCs. (F) Expression analysis of cyclins (*CCNA2*, *CCNB1*, *CCND1*, *CCND2*, *CCNE1*) in *PKHD1*-Hetero and *PKHD1*-KO CCs. Results represent the mean ± SD of 3 separate experiments (2-tailed *t* test). $^{*}p$ <0.05, $^{**}p$ <0.01, $^{***}p$ <0.001. CCs, cholangiocytic cysts; iPS, induced pluripotent stem; *PKHD1*-Hetero, heterozygously mutated *PKHD1; PKHD1*-KO, *PKHD1* knockout; RT-qPCR, quantitative reverse transcription PCR. (This figure appears in colour on the web.)

PKHD-KO CCs, were similar to those in *PKHD1*-Hetero CCs (Fig. 2C, right panel). Expressions of aquaporin 1 (*AQP1*), cystic fibrosis transmembrane conductance regulator (*CFTR*) and *AE2* (or *SLC4A2*) were significantly higher in *PKHD1*-KO CCs compared with *PKHD1*-Hetero CCs (Fig. S2B). These were preferentially localized to the lateral and apical membranes of the cells in *PKHD1*-Hetero CCs, whereas accumulation of these proteins in basal membranes was observed in *PKHD1*-KO CCs (Fig. S2C). Analysis using scanning electron microscopy revealed that the length of primary cilia was shorter in *PKHD1*-KO CCs (~1.8–3.0 μm) compared to that in *PKHD1*-Hetero CCs (~4.9–6.0 μm, Fig. S2D). These data were compatible with the phenotypes of cholangiocytes in rodent models of CHF.[9,15]

The numbers and the sizes of *PKHD1*-KO CCs were significantly greater than those of *PKHD1*-Hetero CCs (Fig. 2A and 2D, left panel) because of the increased numbers of cells that composed the CCs (Fig. 2D, right panel). Both the production of proliferating cell nuclear antigen (PCNA) and expression of cyclin-family genes were significantly increased in *PKHD1*-KO CCs compared with *PKHD1*-Hetero CCs (Fig. 2E and F). These data demonstrated that the proliferation of *PKHD1*-KO iPS-derived cholangiocytes was upregulated similarly to the cholangiocytes in CHF animal models,[16,17] suggesting that this abnormal proliferation mimics the ductal plate malformation observed in the liver of patients with CHF.

IL-8 production promotes the abnormal proliferation of *PKHD1*-KO CCs in an autocrine manner

To investigate the pathophysiology of the abnormal proliferation of cholangiocytes (ductal plate malformation) in CHF, we analyzed the gene expression in iPS-derived CHF-model cholangiocytes, *PKHD1*-KO CCs. Comprehensive analysis using microarray demonstrated that the gene expression pattern in *PKHD1*-KO CCs was different from that in *PKHD1*-Hetero CCs (Fig. 3A, left panel). Pathway analysis using a microarray database indicated that pathways related to cell proliferation were significantly upregulated in *PKHD1*-KO CCs compared with *PKHD1*-Hetero CCs (Table S1 and S2). Interleukin-8 (*IL-8*) exhibited the greatest increase among the humoral factors derived from *PKHD1*-KO CCs. The expression and production

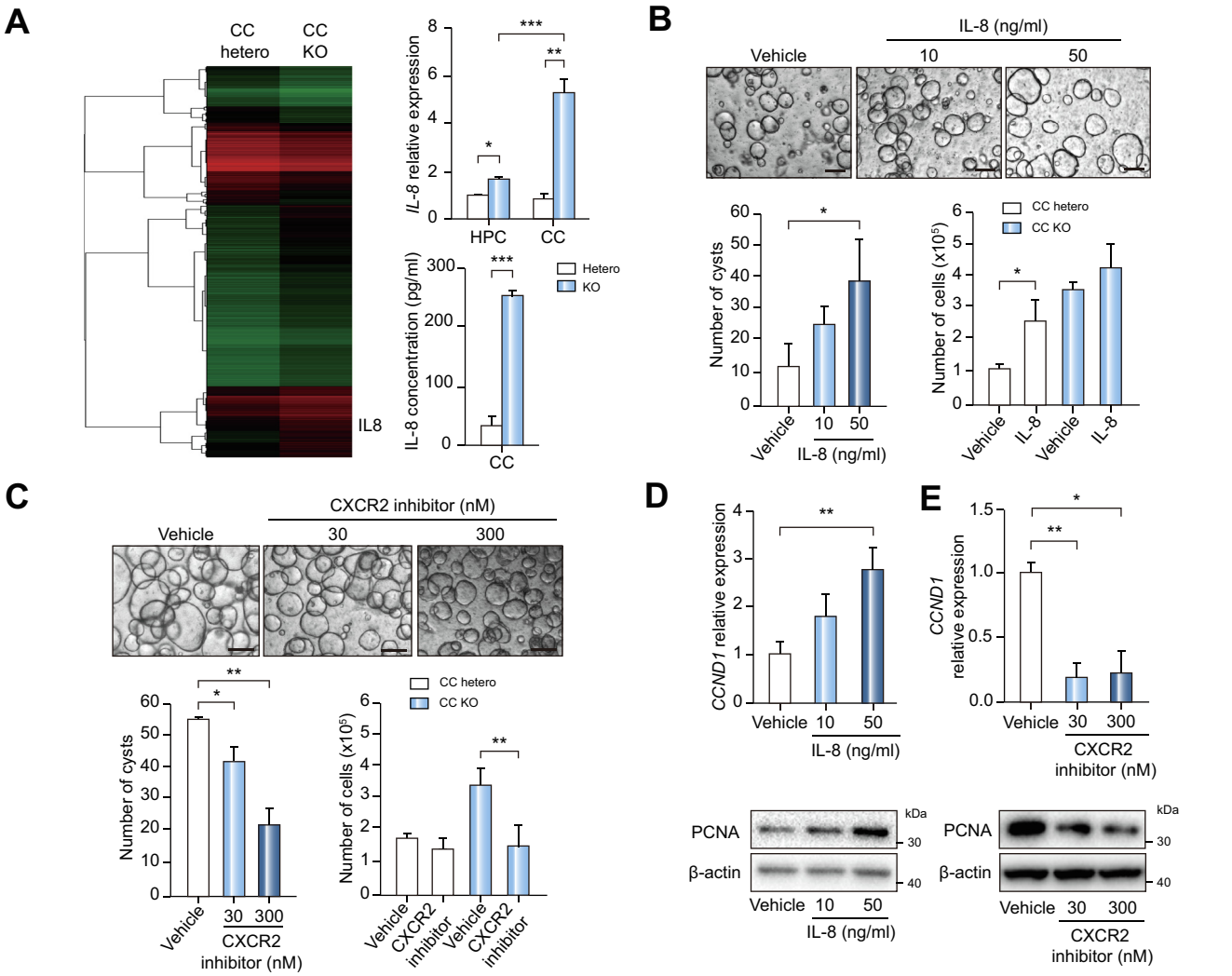

Fig. 3. IL-8 promotes the increased proliferation of *PKHD1*-KO CCs in an autocrine manner. (A) Hierarchical cluster analysis of upregulated or downregulated genes based on cDNA microarray revealed the expression level of IL-8 was increased in *PKHD1*-KO CCs (left panel). RT-qPCR (upper-right panel) and ELISA (lower-right panel) of IL-8 in HPC or CCs demonstrated IL-8 production was significantly increased in *PKHD1*-KO CCs compared with *PKHD1*-Hetero CCs. (B) Representative images of *PKHD1*-Hetero CCs stimulated by human IL-8 (upper panel). Numbers of CCs (lower-left panel) and cells in CCs (lower-right panel) are shown. (C) Representative images of *PKHD1*-KO CCs treated with a CXCR2 (IL-8 receptor) inhibitor (SB225002, upper panel). Numbers of CCs (lower-left panel) and cells in CCs (lower-right panel) are shown. (D) Expression of *CCND1* (upper panel) and immunoblot analysis of PCNA (lower panel) showed that proliferation of cells in *PKHD1*-Hetero CCs was significantly increased by IL-8 stimulation dose-dependently. (E) Expression of *CCND1* (upper panel) and immunoblot analysis of PCNA (lower panel) showed that proliferation of cells in *PKHD1*-KO CCs was significantly decreased by a CXCR2 inhibitor. Results represent the mean ± SD (2-tailed *t* test). $^{*}p$ <0.05, $^{**}p$ <0.01, $^{***}p$ <0.001. Scale bars: 100 μm. CCs, cholangiocytic cysts; HPC, hepatocyte progenitor-like cell; iPS, induced pluripotent stem; *PKHD1*-Hetero, heterozygously mutated *PKHD1;* *PKHD1*-KO, *PKHD1* knockout; RT-qPCR, quantitative reverse transcription PCR. (This figure appears in colour on the web.)

of IL-8 were significantly increased in *PKHD1*-KO CCs (Fig. 3A and Fig. S2E). IL-8 expression in *PKHD1*-KO CCs was significantly upregulated compared with *PKHD1*-KO HPCs (Fig. 3A, upper-right panel). There was no significant difference in IL-8 expression between *PKHD1*-Hetero HPCs and *PKHD1*-Hetero CCs, demonstrating that the upregulation of IL-8 induced by the dysfunction of fibrocystin was enhanced in the cholangiocyte stage relative to the hepatoblast stage. The receptor of IL-8 was expressed on *PKHD1*-Hetero and *PKHD1*-KO CCs (Fig. S2F). The expressions of C-X-C motif chemokine ligand (*CXCL) 1*, *CXCL5*, and *MCP-1 (or CCL2)* were also significantly elevated in *PKHD1*-KO CCs compared with *PKHD1*-Hetero CCs (Fig. S2G).

To determine whether IL-8 is essential for the abnormal proliferation of *PKHD1*-KO CCs, the effects of IL-8 and an IL-8 receptor antagonist on CCs were evaluated. The numbers and the sizes of *PKHD1*-Hetero CCs were increased by IL-8 stimulation (Fig. 3B), whereas those of *PKHD1*-KO CCs were decreased dose-dependently by treatment with a C-X-C motif chemokine receptor (CXCR) 1 antagonist (reparixin, Fig. S3A) or a CXCR2 antagonist (SB225002, Fig. 3C). Cyclin D1 (CCND1) expression in *PKHD1*-Hetero CCs was increased by IL-8 stimulation and was suppressed in *PKHD1*-KO CCs in the presence of the CXCR1 antagonist (Fig. S3A) or the CXCR2 antagonist (Fig. 3D and E). Immunoblot analysis of PCNA revealed that the proliferation of CC cells was regulated in an IL-8-dependent manner (Fig. 3D and E). These data clearly show that autocrine-IL-8 production and the IL-8-CXCR1/2 signaling cascade are necessary for the abnormal proliferation of human cholangiocytes lacking fibrocystin.

Loss of fibrocystin increases IL-8 expression through the activation of MAPK pathway in cholangiocytes

To clarify the molecular mechanisms underlying the upregulated expression of IL-8 caused by the loss of fibrocystin function, we evaluated phosphorylation of the MAPK pathway that was activated in cholangiocytes in a rodent model of CHF.[16,18] Immunoblot analysis of *PKHD1*-KO and *PKHD1*-Hetero CCs revealed that the phosphorylation of ERK (MAPK3), JNK (MAPK8), and c-Jun was upregulated in *PKHD1*-KO CCs compared with *PKHD1*-Hetero CCs, whereas the phosphorylation of p38MAPK in *PKHD1*-KO CCs was similar to that in *PKHD1*-Hetero CCs (Fig. 4A). The total amounts of JNK and c-Jun protein were also increased in *PKHD1*-KO CCs compared with *PKHD1*-Hetero CCs. Gene set enrichment analysis using microarray data also revealed a significant enrichment of ERK-related pathways of MAPK in *PKHD1*-KO CCs (Fig. 4B).

Previous reports showed that *IL-8* expression was regulated by AP-1, formed from c-Jun and c-Fos.[19] The MEK (MAP2K) pathway activates the transcription of AP-1 via Elk-1, which upregulates the protein production of c-Jun.[20] Thus, the relationship between activated MAPK pathways and *IL-8* expression in *PKHD1*-KO CCs was evaluated. Both the numbers of CCs and *IL-8* expression were significantly suppressed in *PKHD1*-KO CCs by 72 h treatment with the selective MEK-1 and MEK-2 inhibitor U0126 (Fig. 4C), which functionally antagonizes AP-1 transcriptional activity.[20] Expression of CCND1 was also significantly suppressed in *PKHD1*-KO CCs by U0126 treatment (Fig. S3B). *IL-8* expression was suppressed in *PKHD1*-KO CCs by U0126 treatment for 24 h, whereas the number of the CCs did not change at this point of time (Fig. 4C). These data demonstrated that the proliferation of cholangiocytes in CCs is suppressed by the MEK/ERK inhibitor in a time-dependent manner, and that the suppression of IL-8 in the CCs does not result from the decreased proliferation itself. *IL-8* expression, numbers of CCs, and CCND1 expression were significantly suppressed in *PKHD1*-KO CCs by a JNK inhibitor for 72 h (SP600125, Fig. 4D and S3C). *IL-8* expression was also suppressed in *PKHD1*-KO CCs by the JNK inhibitor for 24 h, whereas the number of CCs

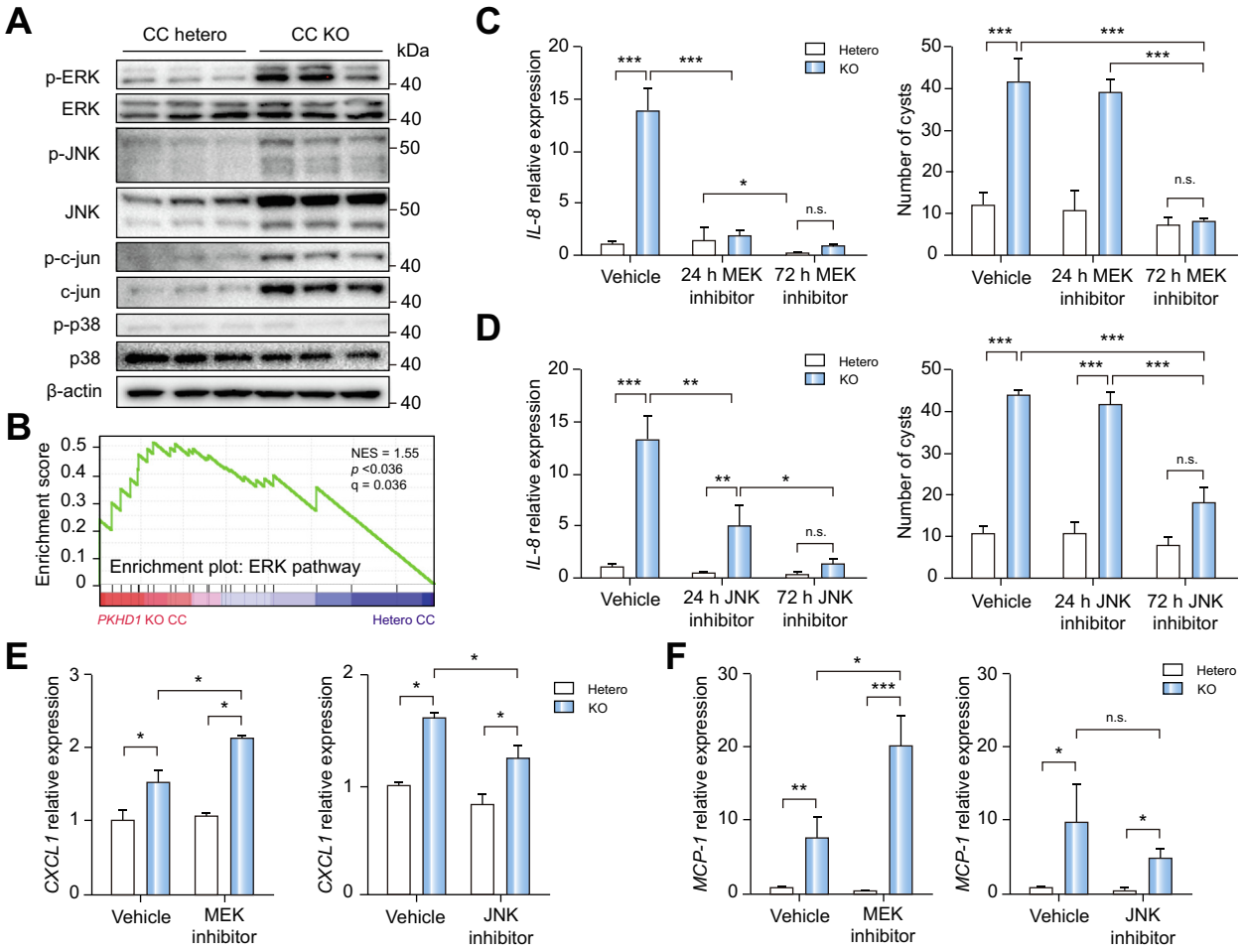

Fig. 4. Loss of fibrocystin increases IL-8 expression in cholangiocytes by activation of mitogen-activated protein kinases. (A) Immunoblot analysis of phosphorylated ERK, phosphorylated JNK, phosphorylated c-Jun, and phosphorylated p38MAPK in *PKHD1*-Hetero and *PKHD1*-KO CCs. (B) Gene set enrichment analysis of ERK pathway signatures was enriched in *PKHD1*-KO CCs. (C) *IL-8* expression and numbers of *PKHD1*-Hetero and *PKHD1*-KO CCs treated with or without MEK inhibitor (10 μM U0126) for 24 h and 72 h. (D) *IL-8* expression and numbers of *PKHD1*-Hetero and *PKHD1*-KO CCs treated with or without JNK inhibitor (10 μM SP600125) for 24 h and 72 h. (E) RT-qPCR analysis of *CXCL1* in *PKHD1*-Hetero and *PKHD1*-KO CCs treated with or without MEK inhibitor (left panel, 10 μM U0126), or JNK inhibitor (right panel, 10 μM SP600125). (F) RT-qPCR analysis of *MCP-1* in *PKHD1*-Hetero and *PKHD1*-KO CCs treated with or without MEK inhibitor (left panel, 10 μM U0126), or JNK inhibitor (right panel, 10 μM SP600125). Results represent the mean ± SD (2-tailed *t* test). $^{*}p$ <0.05, $^{**}p$ <0.01, $^{***}p$ <0.001. CCs, cholangiocytic cysts; iPS, induced pluripotent stem; *PKHD1*-Hetero, heterozygously mutated *PKHD1*; *PKHD1*-KO, *PKHD1* knockout; RT-qPCR, quantitative reverse transcription PCR. (This figure appears in colour on the web.)

did not change (Fig. 4D) as is the case with MEK/ERK inhibitor. Meanwhile, the expression of other chemokines such as *CXCL1* and *MCP-1* was not suppressed by U0126 or SP600125 (Fig. 4E and F). These data showed that the abnormal activation of MAPKs, especially the MEK and JNK pathways, are responsible for the increased expression of *IL-8* and subsequent cell proliferation in fibrocystin-deficient cholangiocytes.

IL-8 increases CTGF production derived from *PKHD1*-KO cholangiocytic cysts

To investigate the relationship between the abnormally increased IL-8 production and fibrotic changes, we analyzed the expression of candidate genes sharing a common transcriptional factor with IL-8 (Fig. S4A-B). Among them, the expression of *CTGF* was significantly elevated in *PKHD1*-KO CCs compared with *PKHD1*-Hetero CCs (Fig. 5A and S4B). ELISA showed that the production of CTGF was significantly increased in *PKHD1*-KO CCs compared with *PKHD1*-Hetero CCs (Fig. 5B and S4B). Transforming growth factor *(TGF)-β1* expression was also elevated in *PKHD1*-KO CCs compared with *PKHD1*-Hetero CCs (Fig. S4C). *CTGF* expression was upregulated in *PKHD1*-Hetero CCs by IL-8 stimulation (Fig. 5C and D) and suppressed in *PKHD1*-KO CCs by treatment with the IL-8 receptor antagonists (Fig. 5E and S4D). The expression of *CTGF* and *TGF-β1* were also suppressed in *PKHD1*-KO CCs by a MEK inhibitor (Fig. 5F and S4E-F). Conversely, the expression of *IL-8* in *PKHD1*-KO CCs was upregulated by CTGF stimulation (Fig. S4G). These data showed that the expression of *IL-8* and *CTGF* in human cholangiocytes lacking fibrocystin are increased by each other, and that a positive feedback mechanism between IL-8 and CTGF is regulated by MAPK activation, including MEK and JNK-c-Jun pathways.

Expression of IL-8 and CTGF are increased in the liver of patients with CHF

To validate the significance of IL-8 and CTGF obtained in the *in vitro* study of CHF using *PKHD1*-KO iPS-derived CCs, liver and serum samples obtained from patients with CHF were analyzed. We retrospectively collected liver tissues and serum samples of patients with clinically diagnosed CHF and chronic hepatitis C (CHC). Liver samples of healthy children cannot be obtained for ethical reasons, and thus samples derived from pediatric patients with CHC were used as controls in this study. The clinical backgrounds of patients with CHF or CHC are shown in Table 1. Liver biopsies were performed for patients with CHF or CHC at the follow-up and before the start of antiviral treatments, respectively. Fibrotic expansion in the portal area and ductal plate malformation were observed in all patients with CHF (Fig. S5). A previous report showed minimal changes in inflammation in the CHF liver;[21] however, it is unclear whether the accumulation of macrophages occurs in the liver of patients with CHF. We evaluated the number of $CD68^+$ macrophages accumulated around the portal area in the liver of patients with CHF and found that it was equivalent to that of patients with CHC (Fig. 6A and B). All patients with CHC exhibited grade 1 portal inflammation based on the Scheuer histological activity index (Fig. S5).

Serum IL-8 levels were significantly higher in patients with CHF than those with CHC after viral eradication (Fig. 6C). The time-course of serum IL-8 was as followed: Patients 1 and 2 underwent liver transplantation at 1 year after their final visit and patient 5 was on the waiting list for liver transplantation. The levels of serum IL-8 in patients with CHF who needed liver transplantation were markedly increased in parallel with progression of the disease (Fig. 6D).

Quantitative analysis of gene expression revealed that the expression of *IL-8* and *CTGF* in the liver of patients with CHF was significantly higher than in those with CHC prior to antiviral treatment (Fig. 6E). However, there was no significant difference in the expression levels of *CXCL1* and *MCP-1* (Fig. S6). *CXCL10* was undetectable in the liver of both patients with CHF and CHC. These data indicated that the increased expression of *IL-8* and *CTGF* in the liver is a characteristic feature of CHF when compared with CHC. Taken together, these results obtained using patient samples demonstrated that abnormally increased *IL-8* expression in the liver was present in patients with CHF, consistent with our *in vitro* human iPS-disease model of CHF.

Discussion

This study reports the first evidence that human IL-8 is an essential molecule for the development of cholangiocyte proliferation in CHF (Figs. 3 and 6). Furthermore, our data revealed

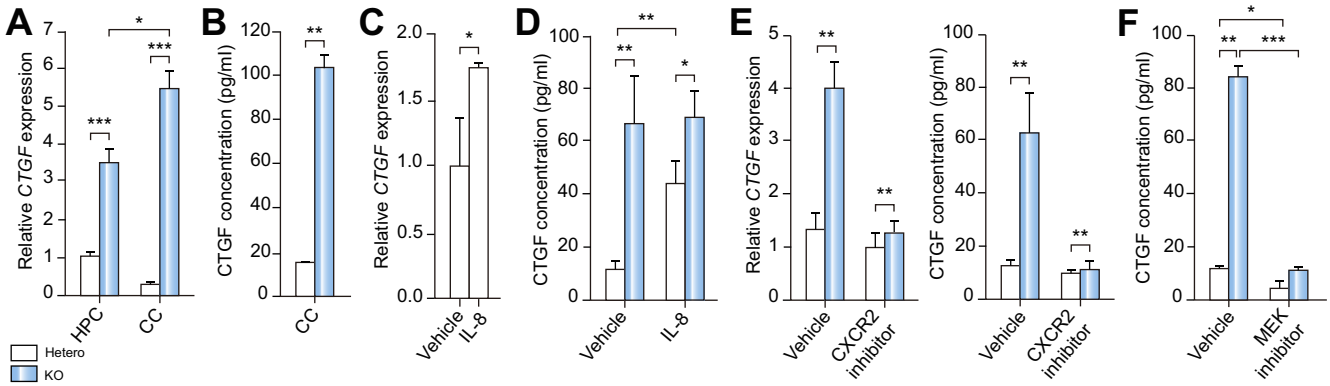

Fig. 5. IL-8 promotes CTGF production derived from *PKHD1*-KO CCs in an autocrine manner. (A) RT-qPCR analysis of *CTGF* in *PKHD1*-Hetero and *PKHD1*-KO cells at the HPC or CC stage. (B) ELISA of CTGF in *PKHD1*-Hetero and *PKHD1*-KO CCs. (C, D) Expression (C) and production (D) of CTGF in *PKHD1*-Hetero CCs with or without IL-8 stimulation. (E) Expression (left panel) and production (right panel) of CTGF in *PKHD1*-Hetero and *PKHD1*-KO CCs treated with or without a CXCR2 inhibitor (300 nM SB225002). (F) ELISA of CTGF in *PKHD1*-Hetero and *PKHD1*-KO CCs with or without a MEK inhibitor (10 μM U0126). Results represent the mean ± SD (2-tailed *t* test). $^*p$ <0.05, $^{**}p$ <0.01, $^{***}p$ <0.001. CCs, cholangiocytic cysts; iPS, induced pluripotent stem; *PKHD1*-Hetero, heterozygously mutated *PKHD1;* *PKHD1*-KO, *PKHD1* knockout; RT-qPCR, quantitative reverse transcription PCR.

Table 1. Clinical characteristics of patients at liver biopsy.

	CHF	CHC	*p* value
Number of patients	7	11	
Male/female	4/3	4/7	n.s.*
Age, median (range)	6 (0–13)	8 (3–19)	n.s.**
AST, U/L, median (range)	36 (24–137)	23 (15–29)	0.024**
ALT, U/L, median (range)	23 (18–107)	18 (13–29)	0.044**
GGT, U/L, median (range)	21 (14–318)	15 (10–20)	n.s.**
Albumin, g/dl, median (range)	4.3 (3.6–4.6)	4.3 (4.1–4.8)	n.s.**
Total bilirubin, mg/dl, median (range)	0.6 (0.3–0.9)	0.5 (0.3–0.9)	n.s.**
Creatine, mg/dl, median (range)	0.3 (0.3–0.6)	0.5 (0.3–0.6)	n.s.**
Platelets, $\times 10^4$/μl, median (range)	12.9 (6.0–26.9)	26.0 (15.6–40.7)	0.004**
PT-INR, median (range)	1.1 (0.8–1.2)	1.0 (0.9–1.1)	n.s.**

CHF, congenital hepatic fibrosis; CHC, chronic hepatitis C; AST, aspartate aminotransferase; ALT, alanine aminotransferase; GGT, gamma-glutamyl transpeptidase; PT-INR, prothrombin time-international normalized ratio; n.s., not significant.
* Fisher's exact probability test.
** 2-tailed *t* test.

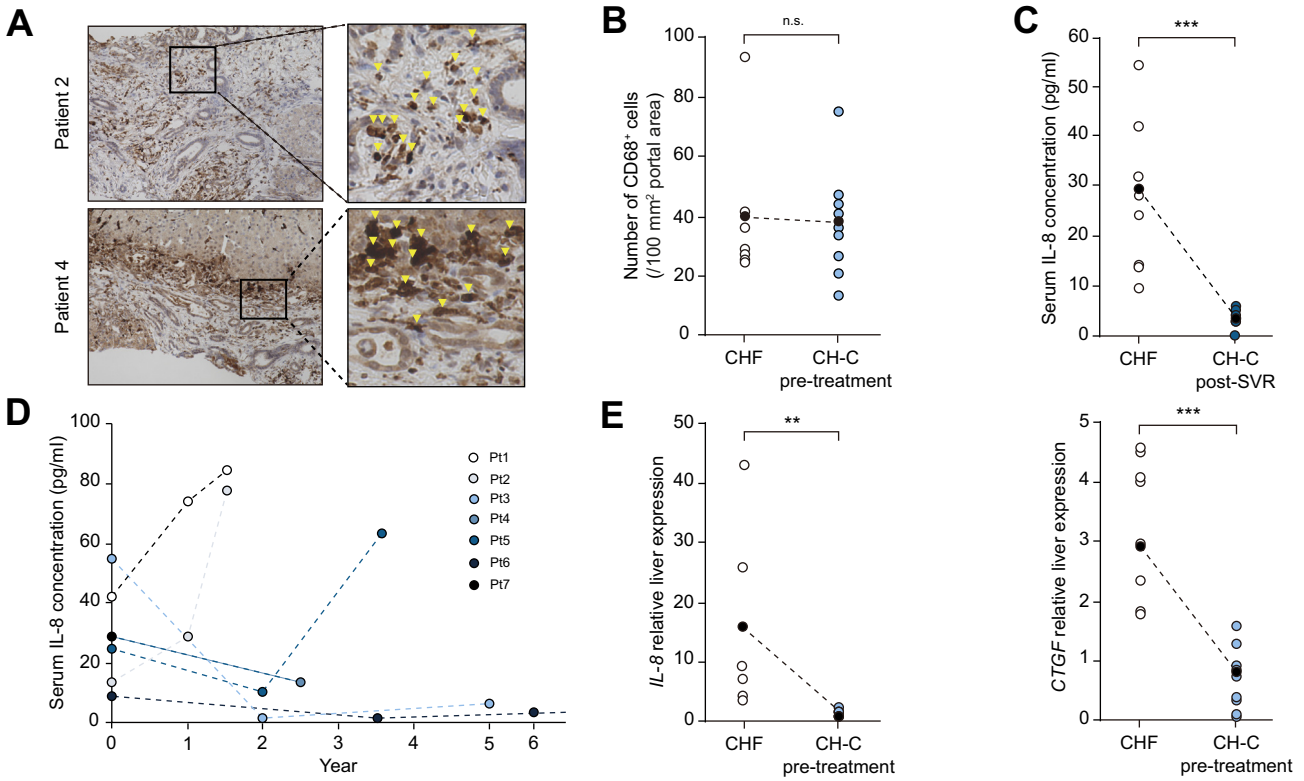

Fig. 6. Increased IL-8 expression in the liver of patients with CHF. (A) Immunostaining of CD68 using liver biopsy samples from pediatric patients with CHF or CHC (pre-treatment). $CD68^+$ macrophages are accumulated in the portal area of pediatric patients with CHF or CHC (arrowhead). (B) Quantitative analysis of the number of $CD68^+$ cells/100 mm^2 portal area in pediatric patients with CHF or CHC. (C) Serum IL-8 in pediatric patients with CHF or CHC post SVR. (D) Time-course of serum IL-8 in patients with CHF. Patients 1 and 2 underwent liver transplantation about 1 year after the final measurement of serum IL-8. (E) Expression analysis of *IL-8* and *CTGF* demonstrated that the expression of these genes is significantly increased in the livers of patients with CHF compared to those with CHC. Results represent the mean ± SD (2-tailed *t* test). $^*p$ <0.05, $^{**}p$ <0.01, $^{***}p$ <0.001. Open circles in dot-plot graphs represent mean of values. CHF, congenital hepatic fibrosis; CHC, chronic hepatitis C; SVR, sustained virologic response. (This figure appears in colour on the web.)

that the production of CTGF, a fibrogenic molecule, is increased in *PKHD1*-KO cholangiocytes in an IL-8-dependent manner (Fig. 5). The phenotype of human iPS-derived cholangiocytes corresponds to intrahepatic cholangiocytes rather than extrahepatic bile ducts, suggesting that our iPS-model can mimic the phenotype of CHF caused by an abnormality of intrahepatic cholangiocytes better than an organoid model derived from human extrahepatic bile ducts.[22] CHF is closely associated with cholangiocyte differentiation during the fetal stage; thus, the investigation of cholangiocytic development from hepatoblasts using a human iPS model might lead to an essential pathophysiological finding. Our data suggested that ductal plate malformation in CHF is caused by the upregulation of cholangiocyte proliferation by IL-8 stimulation in an autocrine manner. The increase in *IL-8* and *CTGF* expression during cholangiocyte differentiation of *PKHD1*-KO iPS cells also indicated that progressive fibrosis in patients with CHF is initiated at the developmental stage of ductal plate formation. These results

from our iPS-model study are consistent with the results of analysis using patient samples. Therefore, our disease model of CHF mimics the pathophysiology of CHF.

The increased cell proliferation and MAPK activation in *PKHD1*-KO cholangiocytes (Fig. 4) were consistent with data from rodent CHF models.[16,18] However, there is no homologous gene to human *IL-8* in rodents. IL-8 is secreted from macrophages and epithelial cells and promotes the proliferation of these cells.[17,23–25] Increased *IL-8* expression in cholangiocytes was reported in several diseases with cholangiocyte damage, including ductular reaction,[25,26] whereas the significance of IL-8 in CHF is unknown. Inflammation was reported to be minimal in CHF compared with chronic hepatitis induced by hepatitis viruses; however, our data show that cholangiocytes lacking the functions of fibrocystin produce inflammatory chemokines, and macrophage accumulation around the portal vein was evident in CHF (Fig. 6). Our data suggest that inflammatory chemokines, secreted by cholangiocytes lacking the functions of fibrocystin, play an important role in the pathophysiology of CHF. Production of CTGF was increased in *PKHD1*-KO cholangiocytes and is highly expressed around the portal area in CHF compared with viral or alcoholic hepatitis.[27] IL-8 and CTGF were abnormally produced in *PKHD1*-KO cholangiocytes via a positive feedback mechanism (Fig. 5). CHF is characterized by progressive hepatic fibrosis without any specific exogenous stimulation; therefore, this positive feedback mechanism may play a central role in the development and progression of CHF.

The activation of MAPK induced by the influx of intracellular calcium with fibrocystin dysfunction has been reported in a murine CHF model.[28] Our data also demonstrated the activation of MEK and JNK-c-Jun pathways in *PKHD1*-KO iPS-derived human cholangiocytes (Fig. 4). This is the first evidence that the MAPKs are activated in human cholangiocytes in the absence of fibrocystin function. The inhibition of MEK activation strongly suppressed *IL-8* and *CTGF* expression compared with the JNK inhibitor, suggesting the MEK inhibitor had a direct inhibitory effect on the expression of *IL-8* and *CTGF*. Taken together, our data demonstrate that the loss of fibrocystin function induces the activation of MAPK pathways and increases the expression of *IL-8* and *CTGF* in human cholangiocytes.

Several data in this study are consistent with the phenotype in CHF rodent models reported previously; however, there are differences between our human data and the phenotype in these models. The expression of *MCP-1*, *CXCL1*, and *CXCL10* were significantly increased in *Pkhd1*-mutant mice compared with control mice, and the infiltration of inflammatory cells around the portal area in *Pkhd1*-mutant mice was quite prominent. CXCL1 is reported to be a functional homolog of human IL-8 in mice.[29] Our data revealed that the expressions of both *IL-8* and *CXCL1* were facilitated in *PKHD1*-KO CCs (Fig. S2), and that *CXCL10* expression was not detected in the liver samples from patients with CHF. The accumulation of $CD68^+$ macrophages around the portal vein in samples from patients with CHF was not severe, but mild as previously reported (Fig. 6A and B).[27] There are 2 possibilities to explain these discrepancies between humans and rodents. One is the difference in cytokine/chemokine profiles between species; there is no gene homologous to human IL-8 in rodents. The other possibility is that some reactions induced by cytokines/chemokines are specific to species and differ between human and rodents. The former is supported by the result that *CXCL10* is highly expressed in murine *Pkhd1*-mutant cholangiocytes but was not detected in our human liver sample. The latter is supported by the result that *CXCL1* and *MCP-1* were expressed in human *PKHD1*-KO CCs (Fig. S2) and liver samples from patients with CHF (Fig. S5).

Liver transplantation is the only established treatment for CHF. This study revealed that an inhibitor of the IL-8 receptor suppressed the abnormal cell proliferation of *PKHD1*-KO cholangiocytes and the expression of CTGF (Figs. 3 and 5). A MEK inhibitor also suppressed the expressions of IL-8 and CTGF in *PKHD1*-KO cholangiocytes. Our data strongly suggest that IL-8, CTGF, and MAPK will be new therapeutic targets for blocking the progression of CHF, and that future clinical trials using drugs targeting such molecules might improve patient survival and reduce the need for liver transplantation in patients with CHF.

Financial support

This work was supported in part by Grants-in-Aid for Scientific Research from the Ministry of Education, Culture, Sports, Science and Technology in Japan (15K08988, 15K08989, 15K15285, 16H05285, 17K09407, 17K19647, 18H02790, and 18K07964).

Conflict of interest

S. Kakinuma and Y. Asahina belong to a donation-funded department funded by Gilead Sciences, AbbVie GK, Chugai Pharmaceutical, Fujirebio, and Merck Sharp & Dohme.

Please refer to the accompanying ICMJE disclosure forms for further details.

Authors' contributions

T.T. performed the experiments and wrote the manuscript. S.K. planned this study, wrote the manuscript, and organized the experiments. M.M., S.K., A.S., and J.T. discussed about the methodology of this study and assisted the experiments of cell culture and flowcytometry. A.K. provided several cell lines and discussed about the strategy of this study. F.K., S.N., M.M, Y.I., M.N., and S.A. discussed about the methodology of this study and technically supported the experiments. T.S., H.K., R.M., A. I. and T.F. collected patients' samples and clinical data, and precisely discussed about the strategy of this study. H.N., Y. A. and M.W. precisely discussed about the strategy of this study, and organized the experiments and the staff for this study.

Acknowledgments

We thank Stem cell bank, Center for Stem Cell Biology and Regenerative Medicine, the University of Tokyo for the gift of the human iPS cell line TkDA3-4. We thank Y. Yamazaki (Division of Stem Cell Therapy, Institute of Medical Science, the University of Tokyo) for excellent technical assistance for FACS. We also thank Prof. Kenjiro Wake (Tokyo Medical and Dental University), Y. Sakamaki, and A. Mimata for helpful discussion and excellent technical assistance for electron microscope.

Supplementary data

Supplementary data to this article can be found online at https://doi.org/10.1016/j.jhep.2019.02.024.

References

Author names in bold designate shared co-first authorship

[1] Desmet VJ. Congenital diseases of intrahepatic bile ducts: variations on the theme "ductal plate malformation". Hepatology 1992;16:1069–1083.

[2] Nakanuma Y, Harada K, Sato Y, Ikeda H. Recent progress in the etiopathogenesis of pediatric biliary disease, particularly Caroli's disease with congenital hepatic fibrosis and biliary atresia. Histol Histopathol 2010;25:223–235.

[3] **Ghodsizadeh A**, Taei A, Totonchi M, Seifinejad A, Gourabi H, Pournasr B, et al. Generation of liver disease-specific induced pluripotent stem cells along with efficient differentiation to functional hepatocyte-like cells. Stem Cell Rev 2010;6:622–632.

[4] Mungenast AE, Siegert S, Tsai LH. Modeling Alzheimer's disease with human induced pluripotent stem (iPS) cells. Mol Cell Neurosci 2016;73:13–31.

[5] Calatayud C, Carola G, Consiglio A, Raya A. Modeling the genetic complexity of Parkinson's disease by targeted genome edition in iPS cells. Curr Opin Genet Dev 2017;46:123–131.

[6] Adeva M, El-Youssef M, Rossetti S, Kamath PS, Kubly V, Consugar MB, et al. Clinical and molecular characterization defines a broadened spectrum of autosomal recessive polycystic kidney disease (ARPKD). Medicine 2006;85:1–21.

[7] Ward CJ, Hogan MC, Rossetti S, Walker D, Sneddon T, Wang X, et al. The gene mutated in autosomal recessive polycystic kidney disease encodes a large, receptor-like protein. Nat Genet 2002;30:259–269.

[8] **Onuchic LF**, **Furu L**, Nagasawa Y, Hou X, Eggermann T, Ren Z, et al. PKHD1, the polycystic kidney and hepatic disease 1 gene, encodes a novel large protein containing multiple immunoglobulin-like plexin-transcription-factor domains and parallel beta-helix 1 repeats. Am J Hum Genet 2002;70:1305–1317.

[9] Masyuk TV, Huang BQ, Ward CJ, Masyuk AI, Yuan D, Splinter PL, et al. Defects in cholangiocyte fibrocystin expression and ciliary structure in the PCK rat. Gastroenterology 2003;125:1303–1310.

[10] **Gallagher AR**, **Esquivel EL**, Briere TS, Tian X, Mitobe M, Menezes LF, et al. Biliary and pancreatic dysgenesis in mice harboring a mutation in Pkhd1. Am J Pathol 2008;172:417–429.

[11] **Locatelli L**, **Cadamuro M**, Spirli C, Fiorotto R, Lecchi S, Morell CM, et al. Macrophage recruitment by fibrocystin-defective biliary epithelial cells promotes portal fibrosis in congenital hepatic fibrosis. Hepatology 2016;63:965–982.

[12] Woollard JR, Punyashtiti R, Richardson S, Masyuk TV, Whelan S, Huang BQ, et al. A mouse model of autosomal recessive polycystic kidney disease with biliary duct and proximal tubule dilatation. Kidney Int 2007;72:328–336.

[13] Zerres K, Mucher G, Becker J, Steinkamm C, Rudnik-Schöneborn S, Heikkilä P, et al. Prenatal diagnosis of autosomal recessive polycystic kidney disease (ARPKD): molecular genetics, clinical experience, and fetal morphology. Am J Med Genet A 1998;76:137–144.

[14] Yanagida A, Ito K, Chikada H, Nakauci H, Kamiya A. An in vitro expansion system for generation of human iPS cell-derived hepatic progenitor-like cells exhibiting a bipotent differentiation potential. PLoS ONE 2013;8 e67541.

[15] Banales JM, Masyuk TV, Bogert PS, Huang BQ, Gradilone SA, Lee SO, et al. Hepatic cystogenesis is associated with abnormal expression and location of ion transporters and water channels in an animal model of autosomal recessive polycystic kidney disease. Am J Pathol 2008;173:1637–1646.

[16] Banales JM, Masyuk TV, Gradilone SA, et al. The cAMP effectors Epac and protein kinase a (PKA) are involved in the hepatic cystogenesis of an animal model of autosomal recessive polycystic kidney disease (ARPKD). Hepatology 2009;49:160–174.

[17] Ren XS, Sato Y, Harada K, Sasaki M, Furubo S, Song JY, et al. Activation of the PI3K/mTOR pathway is involved in cystic proliferation of cholangiocytes of the PCK rat. PLoS ONE 2014;9 e87660.

[18] Sweeney Jr WE, Avner ED. Molecular and cellular pathophysiology of autosomal recessive polycystic kidney disease (ARPKD). Cell Tissue Res 2006;326:671–685.

[19] Bancroft CC, Chen Z, Dong G, Sunwoo JB, Yeh N, Park C, et al. Coexpression of proangiogenic factors IL-8 and VEGF by human head and neck squamous cell carcinoma involves coactivation by MEK-MAPK and IKK-NF-kappaB signal pathways. Clin Cancer Res 2001;7:435–442.

[20] Duncia JV, Santella JB, Higley CA, Pitts WJ, Wityak J, Frietze WE, et al. MEK inhibitors: the chemistry and biological activity of U0126, its analogs, and cyclization products. Bioorg Med Chem Lett 1998;8:2839–2844.

[21] Sato Y, Harada K, Furubo S, Kizawa K, Sanzen T, Yasoshima M, et al. Inhibition of intrahepatic bile duct dilation of the polycystic kidney rat with a novel tyrosine kinase inhibitor gefitinib. Am J Pathol 2006;169:1238–1250.

[22] **Sampaziotis F**, **de Brito MC**, **Madrigal P**, **Bertero A**, **Hannan NRF**, **Vallier L**, et al. Cholangiocytes derived from human induced pluripotent stem cells for disease modeling and drug validation. Nat biotechnol 2015;33:845–852.

[23] Amura CR, Brodsky KS, Gitomer B, McFann K, Lazennec G, Nichols MT, et al. CXCR2 agonists in ADPKD liver cyst fluids promote cell proliferation. Am J Physiol Cell Physiol 2008;294:C786–C796.

[24] Murdoch C, Monk PN, Finn A. Cxc chemokine receptor expression on human endothelial cells. Cytokine 1999;11:704–712.

[25] Isse K, Harada K, Nakanuma Y. IL-8 expression by biliary epithelial cells is associated with neutrophilic infiltration and reactive bile ductules. Liver Int 2007;27:672–680.

[26] Zimmermann HW, Seidler S, Gassler N, Nattermann J, Luedde T, Trautwein C, et al. Interleukin-8 is activated in patients with chronic liver diseases and associated with hepatic macrophage accumulation in human liver fibrosis. PLoS ONE 2011;6 e21381.

[27] Ozaki S, Sato Y, Yasoshima M, Harada K, Nakanuma Y. Diffuse expression of heparan sulfate proteoglycan and connective tissue growth factor in fibrous septa with many mast cells relate to unresolving hepatic fibrosis of congenital hepatic fibrosis. Liver Int 2005;25:817–828.

[28] Masyuk AI, Masyuk TV, Splinter PL, Huang BQ, Stroope AJ, LaRusso NF. Cholangiocyte cilia detect changes in luminal fluid flow and transmit them into intracellular Ca2+ and cAMP signaling. Gastroenterology 2006;131:911–920.

[29] Cacalano G, Lee J, Kikly K, Ryan AM, Pitts-Meek S, Hultgren B, et al. Neutrophil and B cell expansion in mice that lack the murine IL-8 receptor homolog. Science 1994;265:682–684.